PCP
PLANT & CELL PHYSIOLOGY

# *Arabidopsis SMN2/HEN2*, Encoding DEAD-Box RNA Helicase, Governs Proper Expression of the Resistance Gene *SMN1/RPS6* and Is Involved in Dwarf, Autoimmune Phenotypes of *mekk1* and *mpk4* Mutants

Momoko Takagi[1,2,3], Naoki Iwamoto[1], Yuta Kubo[1], Takayuki Morimoto[1], Hiroki Takagi[4,5], Fuminori Takahashi[6], Takumi Nishiuchi[7], Keisuke Tanaka[8], Teruaki Taji[9], Hironori Kaminaka[3], Kazuo Shinozaki[6], Kazuya Akimitsu[1,2], Ryohei Terauchi[4,10], Ken Shirasu[11] and Kazuya Ichimura[1,2,*]

[1]Faculty and Graduate School of Agriculture, Kagawa University, 2393 Ikenobe, Miki-cho, Kita-gun, Kagawa, 761-0795 Japan
[2]United Graduate School of Agriculture, Ehime University, 3-5-7 Tarumi, Matsuyama, Ehime, 790-8566 Japan
[3]Faculty of Agriculture, Tottori University, 4-101 Koyama Minami, Tottori, 680-8553 Japan
[4]Department of Genomics and Breeding, Iwate Biotechnology Research Center, 22-174-4 Narita, Kitakami, Iwate, 024-0003 Japan
[5]Department of Bioproduction Science, Ishikawa Prefectural University, 1-308 Suematsu, Nonoichi, Ishikawa, 921-8836 Japan
[6]Gene Discovery Research Group, RIKEN Center for Sustainable Resource Science, 3-1-1 Koyadai, Tsukuba, Ibaraki, 305-0074 Japan
[7]Institute for Gene Research, Advanced Science Research Center, Kanazawa University, Takaramachi, Kanazawa, Ishikawa, 920-8640 Japan
[8]Nodai Genome Research Center, Tokyo University of Agriculture, 1-1-1 Sakuragaoka, Setagaya-ku, Tokyo, 156-8502 Japan
[9]Department of Bioscience, Tokyo University of Agriculture, 1-1-1 Sakuragaoka, Setagaya-ku, Tokyo, 156-8502 Japan
[10]Laboratory of Crop Evolution, Graduate School of Agricultural Sciences, Kyoto University, Kitashirakawa Oiwake-cho, Sakyo-ku, Kyoto, 606-8502 Japan
[11]Plant Immunity Research Group, RIKEN Center for Sustainable Resource Science, 1-7-22 Suehiro-cho, Tsurumi-ku, Yokohama, Kanagawa, 230-0045 Japan
*Corresponding author: E-mail, kichimura@ag.kagawa-u.ac.jp; Fax, +81-87-891-3021.
(Received 29 April 2020; Accepted 21 May 2020)

**In *Arabidopsis thaliana*, a mitogen-activated protein kinase pathway, MEKK1–MKK1/MKK2–MPK4, is important for basal resistance and disruption of this pathway results in dwarf, autoimmune phenotypes. To elucidate the complex mechanisms activated by the disruption of this pathway, we have previously developed a mutant screening system based on a dwarf autoimmune line that overexpressed the N-terminal regulatory domain of MEKK1. Here, we report that the second group of mutants, *smn2*, had defects in the *SMN2* gene, encoding a DEAD-box RNA helicase. *SMN2* is identical to *HEN2*, whose function is vital for the nuclear RNA exosome because it provides non-ribosomal RNA specificity for RNA turnover, RNA quality control and RNA processing. Aberrant *SMN1/RPS6* transcripts were detected in *smn2* and *hen2* mutants. Disease resistance against *Pseudomonas syringae* pv. *tomato* DC3000 (*hopA1*), which is conferred by *SMN1/RPS6*, was decreased in *smn2* mutants, suggesting a functional connection between *SMN1/RPS6* and *SMN2/HEN2*. We produced double mutants *mekk1smn2* and *mpk4smn2* to determine whether the *smn2* mutations suppress the dwarf, autoimmune phenotypes of the *mekk1* and *mpk4* mutants, as the *smn1* mutations do. As expected, the *mekk1* and *mpk4* phenotypes were suppressed by the *smn2* mutations. These results suggested that *SMN2* is involved in the proper function of *SMN1/RPS6*. The Gene Ontology enrichment analysis using RNA-seq data showed that defense genes were downregulated in *smn2*, suggesting a positive contribution of *SMN2* to the genome-wide expression of defense genes. In conclusion, this study provides novel insight into plant immunity via *SMN2/HEN2*, an essential component of the nuclear RNA exosome.**

**Keywords:** Autoimmunity • DEAD-box RNA helicase • MAP kinase pathway • Nuclear RNA exosome • Posttranscriptional gene regulation • *Pseudomonas syringae* pv. *tomato* DC3000.

## Introduction

Plant immunity comprises pattern-triggered immunity (PTI) and effector-triggered immunity (ETI). Pattern recognition receptors (PRRs) on the cell surface perceive microbe-associated molecular patterns and activate PTI against a broad range of microbes (Dodds and Rathjen 2010, Tsuda and Katagiri 2010, Ranf 2017). Virulent microbial pathogens deploy effectors that suppress PTI and multiply in the plant tissues (Dodds and Rathjen 2010, Asai and Shirasu 2015). The recognition of such effectors by nucleotide-binding domain leucine-rich repeat (NLR) proteins induces ETI, often accompanied by localized cell death, called the hypersensitive response (Cui et al. 2015). The *Arabidopsis thaliana* mitogen-activated protein kinase (MAPK) pathway MEKK1–MKK1/MKK2–MPK4 functions downstream of the PRRs and provides basal resistance against virulent oomycete *Hyaloperonospora arabidopsidis* Noco2 and bacterial pathogen *Pseudomonas syringae* pv. *tomato* DC3000 (Zhang et al. 2012). Disruption of this pathway results in dwarf, autoimmune phenotypes because of constitutive defense

*Plant Cell Physiol.* 61(8): 1507–1516 (2020) doi:10.1093/pcp/pcaa071, available online at https://academic.oup.com/pcp

responses such as spontaneous cell death and accumulation of reactive oxygen species (Qiu et al. 2008, Suarez-Rodriguez et al., 2010). Study with the *mekk1* mutant showed that the dwarf, autoimmune phenotypes are temperature dependent and partially dependent on *RAR1* encoding cochaperon interacting with HSP90 and SGT1 for the stabilization of NLR proteins or *SID2* encoding isochorismate synthase essential for pathogen-induced salicylic acid biosynthesis (Ichimura et al. 2006). Because NLR activation is often suppressed by high temperature and in *rar1* or *sid2* mutants, the loss of *mekk1* has been suggested to activate an NLR pathway(s) (Ichimura et al. 2006). As predicted, screening for genetic suppressors of the dwarf phenotype of *mkk1mkk2* revealed that a coiled-coil-type NLR protein-encoding gene, *SUMM2*, is involved in the dwarf, autoimmune phenotypes caused by the disruption of the MEKK1–MKK1/MKK2–MPK4 pathway (Zhang et al. 2012). The same suppressor screening identified *SUMM1/MEKK2*, *SUMM3/CRCK3* and *SUMM4/MKK6* (Kong et al. 2012, Zhang et al. 2017, Lian et al. 2018). Disruption of the MEKK1–MKK1/MKK2–MPK4 pathway removes MPK4-mediated repression ofSUMM1/MEKK2, the closest paralog of MEKK1, and constitutively activates SUMM2 (Zhang et al. 2017). MPK4 phosphorylates calmodulin-binding receptor-like cytoplasmic kinase 3 (SUMM3/CRCK3) and a decapping enhancer (PAT1), and these proteins also associate with SUMM2 in planta (Roux et al. 2015, Zhang et al. 2017). SUMM3/CRCK3 and PAT1 may serve as a guardee or decoy of SUMM2 (Zhang et al. 2017).

Recently, we generated estradiol-inducible MEKK1N-Myc transformants of Landsberg *erecta* (L*er*) as phenocopies of the *mekk1* mutant. We mutagenizedseeds of the transformants and performed genetic screening to isolate the suppressors of the MEKK1N-Myc overexpression-induced dwarf phenotype. We chose ninemutants with the best dwarfism suppression. The mutant loci were designated *suppressor of MEKK1N overexpression-induced dwarf* (*SMN*) *1* and *SMN2* (Takagi et al. 2019). We have reported the isolation of five mutants belonging to the first complementation group (Takagi et al. 2019). We have identified a locus, designated *SMN1*, encoding the Toll, interleukin-1 receptor, resistance protein (TIR)-class NLR (TNL) protein RPS6, which recognizes the HopA1 effector from *P. syringae* and is required for resistance to this pathogen (Kim et al. 2009, Takagi et al. 2019). Mutations in *SMN1/RPS6* partially suppress the dwarf, autoimmune phenotypes of *mekk1* and *mpk4*. We have suggested that two structurally distinct NLR proteins, SMN1/RPS6 and SUMM2, monitor the integrity of the MEKK1–MKK1/MKK2–MPK4 pathway (Takagi et al. 2019). The mRNA levels of *SMN1/RPS6* are regulated by the nonsense-mediated mRNA decay (NMD) surveillance mechanism that degrades aberrant mRNAs in the processing body (P-body) in the cytosol (Gloggnitzer et al. 2014). Impairment of NMD by the loss of functional mutation in *SMG7*, encoding NMD component, leads to autoimmunity through deregulation of the *SMN1/RPS6* transcript (Gloggnitzer et al. 2014).

In addition to the P-body in the cytosol, the RNA exosome, located in both the cytosol and nucleus, is the major machinery for RNA degradation. The RNA exosome degrades aberrant RNAs in the 3′–5′ direction and is involved in RNA turnover to regulate RNA level, RNA quality control to eliminate defective RNAs, and RNA processing for the maturation of precursor RNAs (Chiba and Green 2009, Jensen 2010, Zhang and Guo 2017). The nuclear RNA exosome requires the interaction with RNA helicases for its function (Sikorska et al. 2017); two related DEAD-box RNA helicases, mRNA transport-defective 4 (MTR4) and HUA enhancer 2 (HEN2), associate with the nuclear RNA exosome in *Arabidopsis* (Lange et al. 2014). MTR4 and HEN2 are closely related to each other;MTR4 localizes mainly in the nucleolus and is required for the degradation of rRNA precursors and rRNA maturation by-products (Lange et al. 2011). In contrast, HEN2, a nucleoplasmic protein, has a distinct function to the MTR4 because HEN2 is dispensable for rRNA maturation. *HEN2* was initially identified in a forward genetic screen for an enhancer of a flower morphology defect in a *hua1hua2* double mutant (Western et al. 2002) designated as enhancers of a weak *agamous* allele *ag-4*. The *HUA1* encodes CCCH zinc finger protein, a member of RNA-binding protein. The HUA2 is a DExH-box RNA helicase, which maintains homeotic B and C gene expression. Accumulation of a misprocessed *AGAMOUS* transcript in the *hen2* mutant suggests that *HEN2* is required for the degradation of aberrant *AGAMOUS* transcripts (Cheng et al. 2003). *HEN2* has also been identified as a genetic suppressor (*SOP3*) of a developmental defect caused by a weak *pas2-1* allele encoding 3 hydroxy acyl-CoA dehydratase, which is essential for the elongation of very-long-chain fatty acids (Hématy et al. 2016).

However, very little is known about whether the nuclear RNA exosome regulates innate immunity in plants. In this study, we found that *SMN2*, identical to *HEN2*, is a novel suppressor of the dwarf, autoimmune phenotypes of the *mekk1* and *mpk4* mutants. We suggest that *SMN2* is required for the proper function of *SMN1/RPS6*.

## Results

### Identification of the *SMN2* gene by MutMap analysis

To gain insight into the autoimmune and severe dwarf phenotypes of the *mekk1* mutant and to avoid the difficulty of propagating the *mekk1* homozygous mutant, we generated estradiol-inducible MEKK1N-Myc transformants of L*er* as phenocopies of the *mekk1* mutant based on the prediction of a dominant negative effect of the N-terminal regulatory domain (s) because deletion of this domain of the group A plant MAPKKKs converted them into a constitutive active form (Kovtun et al. 2000, Asai et al. 2002, del Pozo et al. 2004) suggesting a negative role of N-terminal regulatory domain. In addition, MEKK1 interacts with the MPK4 through the N-terminal regulatory domain of MEKK1 (Ichimura et al. 1998). Overexpression of MEKK1N may remove MPK4 from the signaling complex, resulting in the loss of function of the MEKK1–MKK1/MKK2–MPK4 pathway. Using this transgenic line, we performed genetic suppressor screening to identify gene(s)

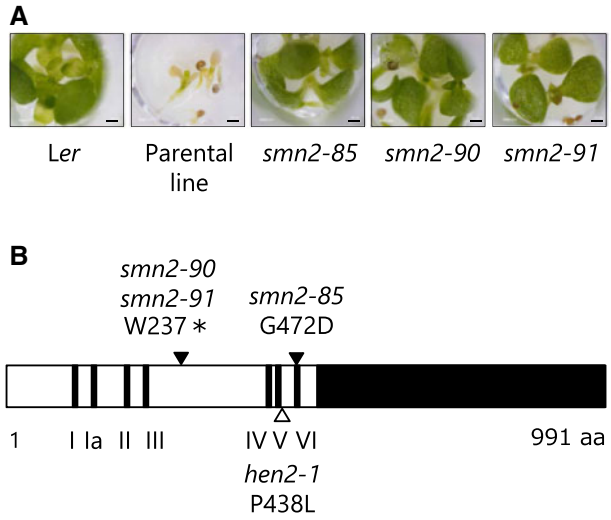


Fig. 1 Identification of the gene mutated in *smn2* mutants. (A) Unlike the parental line, *smn2* mutants do not show the dwarfism induced by MEKK1N overexpression. Seeds of the WT (*Ler*), the parental line for mutant screening, and *smn2* mutants carrying the estradiol-inducible MEKK1N-Myc transgenes were germinated in liquid germination medium (GM) containing 20 $\mu$g/ml estradiol on filter paper for 10 d. Bars = 0.5 mm. (B) Diagram of the SMN2/HEN2 protein. Black bars, helicase motifs I–VI. Triangles, amino acid substitutions encoded by *smn2* alleles (closed) and *hen2-1* (open); individual allele numbers are shown. Asterisk, stop codon. Black box on the right, C-terminal domain.

involved in the autoimmune and severe dwarf phenotypes of the *mekk1* mutant. Here, we report three mutants belonging to the second complementation group: *smn2-85*, *smn2-90* and *smn2-91* (**Fig. 1A**). To find the causal suppressor gene, we backcrossed the three mutants to the parental line, the estradiol-inducible MEKK1N-Myc transgenic *Ler*, and produced F2 individuals from backcross 1 generation with the *smn* phenotype, which were then subjected to a MutMap analysis (Abe et al. 2012). We found that *smn2-90* and *smn2-91* shared almost all of the single nucleotide polymorphisms (SNPs). Because these mutants came from an identical the same M2 seed batch, we concluded that *smn2-90* and *smn2-91* are siblings. In the MutMap analysis, the *smn2* mutants shared the highest peak of the SNP index on chromosome 2 (**Supplementary Fig. S1**). *At2g06990* was the only gene in which nonsynonymous mutations were found in all *smn2* alleles and was thus identified as *SMN2* (**Fig. 1B**). The *smn2-85* mutant had a G472D amino acid substitution, and both *smn2-90* and *smn2-91* carried a nonsense mutation resulting in a change in W237 to a stop codon (**Fig. 1B**). We designed cleaved amplified polymorphic sequence (CAPS) markers for *smn2-85* (**Supplementary Table S1**) and SNP-specific PCR markers for *smn2-90* (**Supplementary Table S2**). Using these markers, we removed the estradiol-inducible MEKK1N-Myc transgene by crossing for further analyses.

## Tissue-specific expression of *SMN2*

In the *mekk1* mutants, cell death and $H_2O_2$ accumulation were observed in the vasculature (Ichimura et al. 2006). Therefore, we

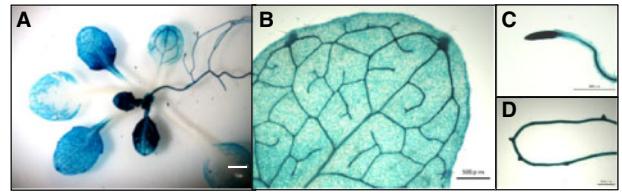


Fig. 2 Tissue-specific expression of *SMN2*. A 1.6-kb promoter region of *SMN2* was transcriptionally fused to the *GUS* reporter gene. The *SMN2* promoter::*GUS* transgenic seeds were germinated and grown on GM medium, and 3-week-old seedlings were stained with X-gluc. One representative out of 12 independent lines is shown. (A) Whole seedling; bar = 1.0 mm. (B) True leaf; bar = 500 $\mu$m. (C) Root tip; bar = 500 $\mu$m. (D) Lateral root primordia; bar = 500 $\mu$m.

investigated whether *SMN2* is expressed in the vasculature. A 1.6-kb DNA fragment containing the *SMN2* promoter was transcriptionally fused to the *GUS* reporter gene and introduced into wild-type (WT) *Ler*. The GUS reporter was expressed predominantly in the vascular tissues, especially in expanded cotyledons and true leaves (**Fig. 2A, B**). Expression of GUS in mesophyll cells was also visible in emerging true leaves and to a lesser extent in expanded leaves (**Fig. 2A**). This *SMN2* expression pattern overlapped with tissue-specific expression of *MEKK1* (Ichimura et al. 2006). These results suggested a role of *SMN2* in the autoimmune phenotype of *mekk1*. We also found strong GUS expression in the root tip, root stele and lateral root primordia (**Fig. 2C, D**).

## Aberrant expression of *SMN1/RPS6* in *smn2* mutants

*HEN2* encodes a component of the nuclear RNA exosome targeting complex (Lange et al. 2014). To find whether the expression of any defense genes is altered in the *smn2* mutants, we checked the data obtained by the tilling array analysis of the *hen2* mutant to elucidate target transcripts degraded by the nuclear RNA exosome (Lange et al. 2014). *SMN1/RPS6* was among the 18 defense genes upregulated in the *hen2* mutant (**Supplementary Table S3**). The *hen2* mutant accumulated an alternative 3′-end transcript and a read-through transcript of *SMN1/RPS6*. We then asked whether aberrant transcripts can be detected in the *smn2* mutants. In the course of Gene Ontology (GO) enrichment analysis (described below), we mapped sequence reads on the *SMN1/RPS6* gene and observed a significant increase in the number of reads at the 3′ untranslated region (UTR) and downstream intergenic regions in *smn2-90* in comparison with *Ler* (**Supplementary Fig. S2**). RT-qPCR analysis with primers to amplify the regions corresponding to the probes used in the tilling array analysis (**Fig. 3A**) confirmed the upregulation of *SMN1/RPS6* transcripts at the 3′ UTR and downstream intergenic regions in the *smn2-85* and *smn2-90* mutants and *hen2-1*, a mutant originally isolated from *Ler* and allelic to *smn2* (**Fig. 3B**) (Western et al. 2002). Transcript levels in these mutants were almost five times that in Ler at site A, seven times at site B and >40 times at site C (**Fig. 3B**). By contrast, the differences between *Ler* and the mutants in the levels of *SMN1/RPS6* transcripts corresponding to the TIR,

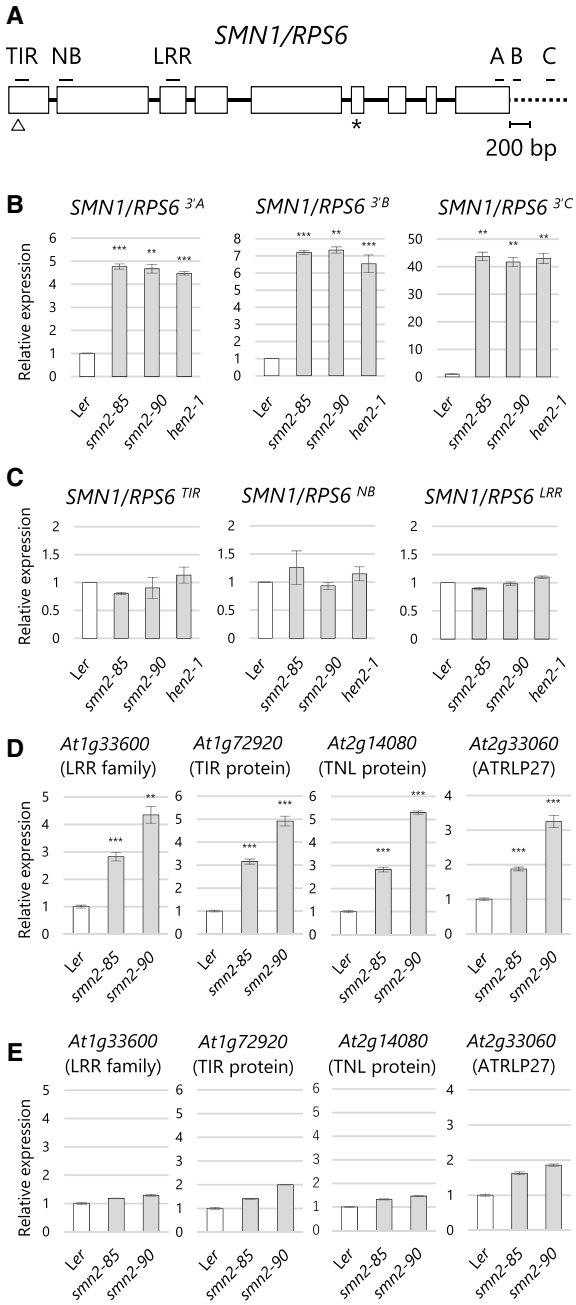


Fig. 3 Detection of aberrant transcripts corresponding to 3′ regions of *SMN1/RPS6* and affected defense genes in *smn2* and *hen2-1* mutants. (A) Diagram of the *SMN1/RPS6* gene. Open boxes, exons; lines, introns; broken line, 3′ intergenic region; open triangle, initiation codon; asterisk, stop codon. Bars above the TIR, NB and LRR domains correspond to the RT-qPCR amplicons. Bars under letters 'A', 'B' and 'C' correspond to the RT-qPCR amplicons of the 3′ UTR (A) and further downstream intergenic regions B and C. (B and C) Detection of aberrant transcripts corresponding to 3′ UTR and further downstream intergenic regions of (B) *SMN1/RPS6* (regions A–C) and (D) defense genes in the *smn2* and *hen2* mutants. (C) Transcripts encoding the TIR, NB and LRR domains of SMN1/RPS6. (E) Transcripts of the coding regions of affected defense genes. Transcript levels are shown relative to those in *Ler* as determined by RT-qPCR using *Actin2* as an internal standard. Plants were grown for 10 or 14 d at 22°C. Error bars, SD ($n = 3$). Representative results from three independent experiments are shown. $P < 0.005$, $P < 0.001$ vs. *Ler* (Student's *t*-test).

nucleotide-binding (NB) and leucine-rich repeat (LRR) domains were not significant (**Fig. 3C**). This result also suggests a possible functional connection between *SMN1/RPS6* and *SMN2/HEN2* via a posttranscriptional mechanism.

Based on the results of the tilling array analysis (Lange et al. 2014; **Supplementary Table S3**), we selected some other representative defense genes, which encode an LRR family protein (*At1g33600*), TIR protein (*At1g72920*), TNL protein (*At2g14080*) and ATRLP27 (*At2g33060*). Using RT-qPCR, we confirmed the accumulation of aberrant transcripts at the 3′-end regions (**Fig. 3D**), but not the coding regions of these genes, in *smn2* mutants (**Fig. 3E**). We also analyzed transcript levels of the *SUMM2* coding region near the 3′ end because this gene has no 3′ UTR. The *SUMM2* transcript levels in the *smn2* and *hen2* mutants were 1.3–1.4 times those in *Ler* (**Supplementary Fig. S3**). Our results confirmed the generation of aberrant transcripts at the 3′ regions of defense genes, including *SMN1/RPS6*, in *smn2* mutants.

## The *smn2* mutations result in the loss of function of *SMN1/RPS6*

We checked whether abnormal expression of *SMN1/RPS6* in the *smn2* mutants alters resistance conferred by *SMN1/RPS6* encoding TNL protein recognizing *P. syringae* HopA1 effector. We inoculated the *smn2-85* and *smn2-90* mutants with *P. syringae* pv. *tomato* (*Pst*) DC3000 (*hopA1*). We used *smn1–150* as a positive control for the loss of resistance. Bacterial growth was highest in *smn1–150*, and was significantly higher in *smn2-85* and *smn2-90* than in *Ler* (**Fig. 4A**), suggesting that *smn2* mutations resulted in the loss of function of *SMN1/RPS6*. We also inoculated the *smn1* and *smn2* mutants with *Pst* DC3000 as the control for *Pst* DC3000 (*hopA1*). Disease resistance against *Pst* DC3000 was not altered in *smn1* and *smn2* mutants compared to *Ler* (**Fig. 4B**).

## Genome-wide identification of defense genes affected by *smn2* mutations

Using *Ler* and *smn2-90*, we performed RNA-seq analysis and detected 250 differentially expressed genes (DEGs). Of those, 86 DEGs were downregulated in *smn2-90*. To elucidate the function of the downregulated genes, we performed GO enrichment analysis with the agriGO. We found that the downregulated genes were involved in response to a stimulus (GO:0050896), response to stress (GO:0006950) and defense response (GO:0006952) (**Supplementary Fig. S4**). To confirm the downregulation of defense genes in *smn2* mutants, we examined four representative genes, *ECS1* (At1G31580), *FMO1* (At1G19250), *WRKY54* (At2G40750) and *WRKY70* (At3G56400), by RT-qPCR with the promiers correspond to the coding regions. The expression levels of *ECS1*, *FMO1*, *WRKY54* and *WRKY70* in *smn2* mutants were reduced to ~40%, 40–56%, 56–70% and 56% in *smn2* mutants, respectively (**Fig. 5**). These data suggested a positive contribution of *SMN2* to the genome-wide expression of defense genes.

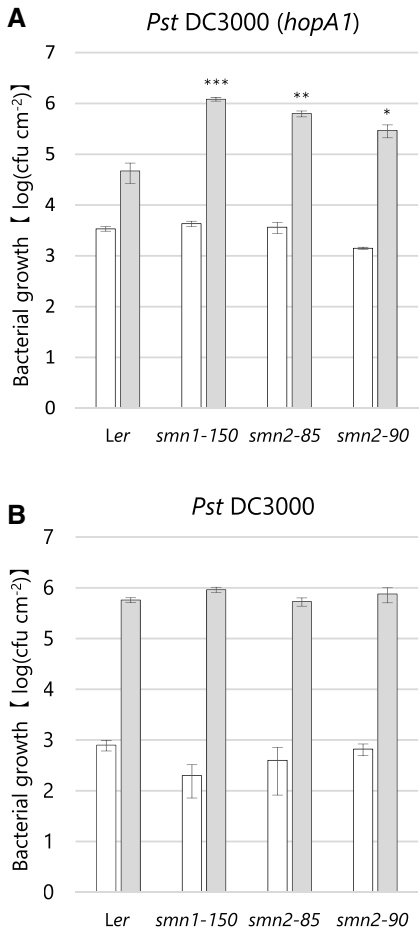


Fig. 4 Population growth of (A) *Pst* DC3000 (*hopA1*) and (B) *Pst* DC3000 in *smn2* mutants. Plants (7–8 weeks old) were inoculated at $1 \times 10^5$cfu/ml (A) or $5 \times 10^4$cfu/ml (B). Values are averages for leaf tissue 0 d (white bar) and 3 d (gray bar) after inoculation. Error bars, SD ($n = 3$). This experiment was performed three times with similar results. $P < 0.05$, $P < 0.01$, $P < 0.001$ vs. *Ler* (Student's *t*-test).

## Suppression of dwarf, autoimmune phenotypes of *mekk1* by *smn2* and *hen2* mutations

To test whether *SMN2* is involved in the dwarf, autoimmune phenotypes of *mekk1*, we generated *mekk1smn2* double mutants. We also used *hen2-1* to increase the accuracy of phenotype analyses. The dwarf phenotype of the *mekk1* mutant was partially suppressed in the *mekk1smn2* and *mekk1hen2* double mutants at 26°C (**Fig. 6A**). To test whether autoimmune phenotype accompanied by cell death and $H_2O_2$ accumulation in *mekk1* were also suppressed in *mekk1smn2* and *mekk1hen2*, we stained leaf tissues with trypan blue to see cell death or diaminobenzidine (DAB) to see $H_2O_2$ accumulation. Fewer cells were stained with trypan blue or DAB in *mekk1smn2* and *mekk1hen2* than in *mekk1* at 26°C (**Fig. 6B, C**). In particular, far fewer cells were stained with trypan blue in the mesophyll of *mekk1smn2* and *mekk1hen2* (**Fig. 6B**). Consistently, DAB staining in the vasculature and adjacent cells of *mekk1* plants

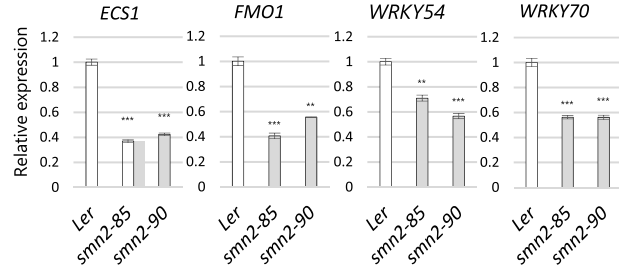


Fig. 5 Expression levels of representative defense genes are reduced in *smn2* mutants. Plants were grown for 10 d at 22°C. Transcript levels are shown relative to *Ler* as determined by RT-qPCR using *Actin2* as an internal standard. Error bars, SD ($n = 3$). Representative results from three independent experiments are shown. $P < 0.01$, $P < 0.001$ vs. *Ler* (Student's *t*-test).

was also suppressed by the *smn2* or *hen2* mutations (**Fig. 6C**). In the case of the *hen2* mutant, we observed darker staining in the vasculature. Upon closer examination, however, several brown tiny dots on the *mekk1hen2* leaf correlated with trypan blue-stained cells were not observed in *hen2*. In conclusion, our data suggest that *SMN2* is involved in the dwarf, autoimmune phenotypes of *mekk1*.

## Suppression of dwarf, autoimmune phenotypes of *mpk4* by *smn2* and *hen2* mutations

*SMN1* is involved in the dwarf, autoimmune phenotype of *mpk4* (Takagi et al. 2019). To examine whether the *smn2* and *hen2* mutations suppress the *mpk4* phenotypes, we produced *mpk4smn2-85* and *mpk4hen2-1* double mutants. The double-mutant plants were clearly larger than the *mpk4* plants but smaller than *Ler*, *smn2*, or *hen2* plants at 24°C (**Fig. 7A**). Consistently, cell death and $H_2O_2$ accumulation were partially suppressed in the *smn2* and *hen2* mutants in comparison with those of *mpk4* at 22°C (**Fig. 7B, C**). These results showed that *SMN2* is involved in the dwarf, autoimmune phenotypes of *mpk4*.

## Discussion

We have previously reported that loss of function of *SMN1/RPS6*, encoding a TNL immune receptor, partially suppressed the dwarf, autoimmune phenotypes of the *mekk1* and *mpk4* mutants, and suggested that SMN1/RPS6 monitors the integrity of the MEKK1–MKK1/MKK2–MPK4 pathway (Takagi et al. 2019). In this study, we found that *SMN2* is identical to *HEN2* and is the causal gene of the second complementation group of the *smn* mutants. We found that disease resistance conferred by *SMN1/RPS6* was decreased by the mutations in *SMN2/HEN*. The *smn2* and *hen2* mutations also partially suppressed the dwarf, autoimmune phenotypes of *mekk1* and *mpk4*. We propose that *SMN2* is involved in the dwarf, autoimmune phenotypes caused by disruption of the MEKK1–MKK1/MKK2–MPK4 pathway by regulating *SMN1/RPS6* expression.

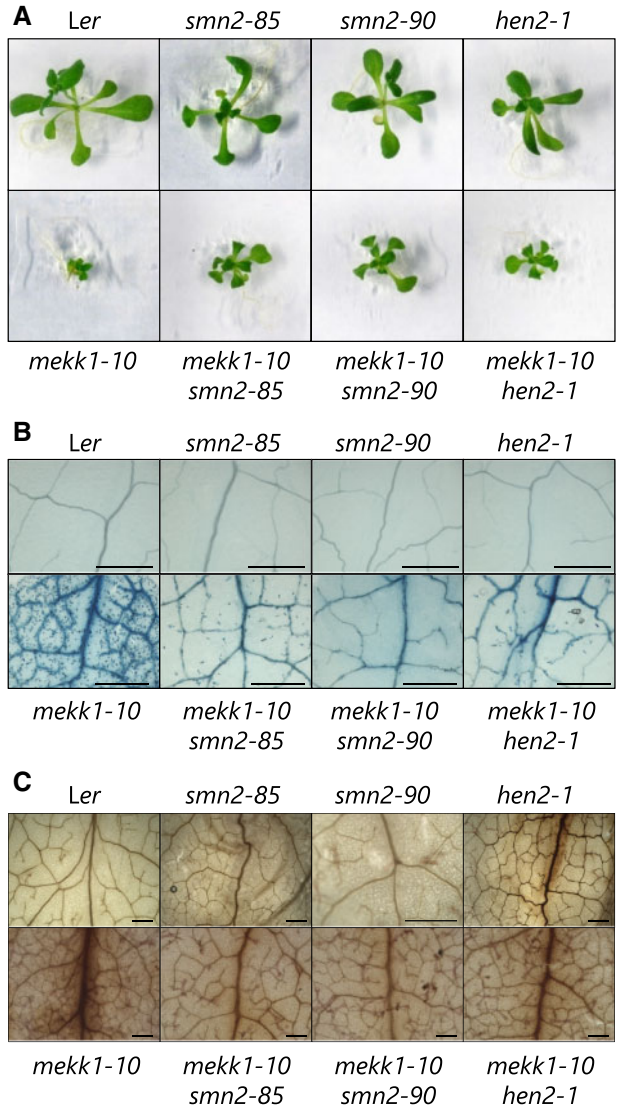


Fig. 6 Dwarf, autoimmune phenotypes of the *mekk1* mutant are partially suppressed by the *smn2* and *hen2* mutations. (A) Morphology, (B) cell death and (C) $H_2O_2$ production. Plants were grown on GM agar for (A) 18 d or (B and C) 14 d at 26°C. Detached true leaves were stained with (B) trypan blue or (C) DAB. Bars = 500 $\mu$m. Data are representative of at least four biological replicates.

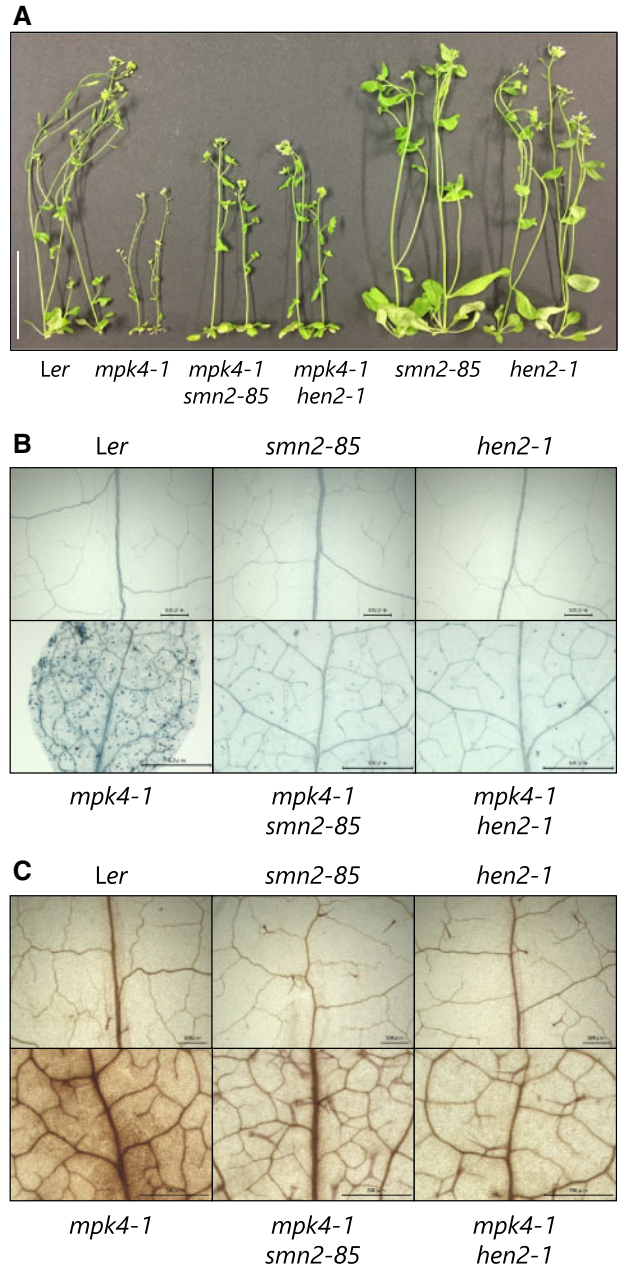


Fig. 7 Dwarf, autoimmune phenotypes of the *mpk4* mutant are partially suppressed by the *smn2* and *hen2* mutations. (A) Morphology, (B) cell death and (C) $H_2O_2$ production. In (A), seeds were germinated on GM for 10 d and, then, the plants were grown in soil at 24°C until 1 month of age. Bar = 5 cm. In (B) and (C), plants were grown in soil for 1 month at 22°C. Detached leaves were stained with (B) trypan blue or (C) DAB. Bars = 500 $\mu$m. Data are representative of three biological replicates.

## Identification of *SMN2*/*HEN2*

Among the suppressor mutants of the dwarf, autoimmune phenotype induced by conditional overexpression of the N-terminal regulatory domain of MEKK1, we have chosen the nine best-scoring mutants: five *smn1*/*rps6* (Takagi et al. 2019), three *smn2*/*hen2* (this study) and a distinct mutant (to be reported elsewhere). As the *smn2-90* and *smn2-91* mutants originated from the same parent, the *smn2* mutants were actually represented by two alleles, *smn2-85* and *smn2-90*. Fewer *smn2* alleles compared to five *smn1* alleles may correspond to the degree of contribution of *SMN1* and *SMN2* to the dwarf phenotype of MEKK1N-Myc-expressing plants. Sequence analysis showed that *smn2-85* had a G472D amino acid substitution and that both *smn2-90* and *smn2-91* carried a nonsense mutation resulting in a stop codon instead of W237. The residue mutated in *smn2-85* is the first of the two glycines in the highly conserved motif VI ($Y_{467}$IQMSGRAGR$_{476}$), required for RNA binding and ATP hydrolysis (Pause et al. 1993, Aubourg et al. 1999). An in vitro binding assay of the yeast initiation factor 4A (eIF-4A), a DEAD-box RNA helicase, suggested that R362 in motif VI is essential for interaction to both RNA and ATP (Pause et al. 1993). The R362 residue of the yeast eIF-4A corresponds to R473 in motif VI of SMN2/HEN2. The G472D substitution in *smn2-85*

adjacent to this critical amino acid could alter charge distribution in motif VI, possibly hampering the interaction with both RNA and ATP. The nonsense mutation in *smn2-90* and *smn2-91* between motifs III and IV is also very likely to cause the loss of function of SMN2/HEN2.

## Possible connection between nuclear RNA exosome and defense responses

The nuclear RNA exosome contains a nine-subunit core (Exo9). Six subunits are similar to RNase PH, but the Exo9 in yeast and humans has lost the active sites, and Rrp44 is tightly associated with Exo9 to degrade RNA (Jensen 2010). *Arabidopsis* Exo9 has RNase activity but requires the interaction with exosome-associated DEAD-box RNA helicases for its function (Sikorska et al. 2017). In *Arabidopsis*, two related DEAD-box RNA helicases, MTR4 and HEN2, associate with the nuclear RNA exosome (Lange et al. 2011). In contrast to MTR4, HEN2 is important for the degradation of non-ribosomal RNAs (Lange et al. 2014). Loss of function of *HEN2* results in the accumulation of polyadenylated nuclear RNAs (exosome substrates) such as short transcripts derived from mRNA genes, 3′-extended mRNAs, incompletely spliced mRNAs, snoRNA and miRNA precursors, and spurious transcripts produced from pseudogenes and intergenic regions (Lange et al. 2014).

In this work, we detected aberrant transcripts of the 3′ UTR of *SMN1/RPS6* in the *smn2-90* mutant (**Supplementary Fig. S2**), but no differences in the levels of coding region transcripts (**Fig. 3C**). We also validated the occurrence of aberrant RNA derived from the 3′ regions of 4 genes (**Fig. 3D**) selected from among 18 defense genes (**Supplementary Table S3**) detected in the tilling array analysis with *hen2* by Lange et al. (2014). Our GO enrichment analysis with the RNA-seq data showed that the majority of genes downregulated in *smn2-90* were stress and/or defense related, suggesting that *SMN2/HEN2* has broad role(s) in mRNA degradation or RNA processing in response to such stimuli. However, inoculation of the *smn2* mutants and L*er* with *Pst* DC3000 resulted in similar disease resistance (**Fig. 4B**). The effect of *smn2* mutations on defense gene expression may be below the threshold to alter disease resistance or may become detectable with other pathogens. Our findings unveil a possible function of SMN2/HEN2 in posttranscriptional gene regulation in biotic stress responses in plants.

Knowledge about connection between nuclear RNA exosome and defense responses has been very limited. The barley *RRP46* gene, encoding a component of the RNA exosome, is responsible for the phenotype of the *Blumeria graminis* f. sp. *hordei* (*Bgh*)-*induced tip cell death1* (*bcd1*) mutant (Xi et al. 2009). Deletion or knockdown of this gene results in infection-induced tip cell death regardless of *Bgh* isolate, suggesting a potential link between RNA exosome and defense responses. Although the *Arabidopsis* mutant phenotypes of *RRP46* (At3G46210) and its paralog (At2g07110) have not been reported, our findings together with this report suggest a functional connection between nuclear RNA exosome and defense responses.

## 3′ region-derived aberrant transcripts normally degraded by nuclear RNA exosome abolish the function of *SMN1/RPS6*

The *smn2* and *hen2* mutations led to a production of abnormal mRNAs relevant to the phenotypes of the *agamous* (Cheng et al. 2003) and *pas2-1* mutants (Hématy et al. 2016). The *hen2-1* mutant accumulates aberrant *AGAMOUS* transcripts containing at least the first intron and a large portion of the second intron, suggesting that *HEN2* is involved in the degradation of misprocessed *AGAMOUS* transcripts (Cheng et al. 2003). The *pas2-1* mutation results in *pas2-1* mRNA variants that are degraded by the nuclear RNA exosome. In the double *pas2-1 suppressor of pas2-1* (*sop*) *3* mutant, one of the *pas2-1* mRNA isoforms producing functional PAS2 protein was stabilized, resulting in the restoration of the developmental defect; the gene mutated in *sop3* is identical to *HEN2* (Hématy et al. 2016). The *smn2* and *hen2* mutations resulted in the production of short *SMN1/RPS6* transcripts from the 3′ UTR and downstream intergenic regions (**Supplementary Fig. S2**), which are normally degraded by the nuclear RNA exosome (this study and Lange et al. 2014), leading to the loss of function. This phenomenon is distinct from the cases of *AGAMOUS* and *pas2-1*. Although the exact step between the transcription and translation of *SMN1/RPS6* affected by the 3′ region-derived aberrant RNAs needs to be elucidated, a plausible explanation for the loss of function is that excess aberrant transcripts may reduce the relative population of the intact *SMN1/RPS6* circular mRNA for translation. A eukaryotic mRNA normally forms the circular structure mediated by the interaction of eIF-4E, 5′ CAP binding protein, and Pab1p, a poly(A) binding protein to promote translation efficiency after mRNA maturation (Tarun and Sachs 1996, Hong et al. 2017). The excess aberrant transcripts of *SMN1/RPS6* may lead to low translation efficiency resulting in the loss of function because of the possibly lowered level of SMN1/RPS6 protein.

The 3′ UTRs of mRNAs regulate their localization, translation and stability. Dehydration stress extends the mRNA 3′ UTRs of a subset of stress-related genes, and the extended 3′ UTRs act as repressors or activators, or lead to read-through transcription (Sun et al. 2017). An RNA-binding polyadenylation regulatory factor, FPA, contributes to the extension of 3′ UTR. FPA negatively regulates flg22-induced reactive oxygen species burst and disease resistance against *Pst* DC3000 by producing different isoforms of the defense-related transcriptional repressor ERF4 through choosing alternative polyadenylation sites (Lyons et al. 2013). The transcript level of *ERF4* is increased in *hen2-1* (Lange et al. 2014).Thus, the stress-induced extension of 3′ UTRs of mRNA may happen not only in response to dehydration, and SMN2/HEN2 might contribute to these phenomena and finely tune stress-regulated gene expression.

## Suppression of dwarf, autoimmune phenotypes of *mekk1* and *mpk4* by *smn2* and *hen2* mutations

We have previously suggested that SMN1/RPS6 is required for monitoring the MEKK1–MKK1/MKK2–MPK4 pathway (Takagi et al. 2019). Disruption of this pathway by pathogen effector(s)

or by T-DNA or transposon insertion activates SMN1/RPS6 and SUMM2 and induces dwarfism and constitutive defense responses (Takagi et al. 2019). In this study, we showed that the *smn2* and *hen2* mutations resulted in the loss of function of *SMN1/RPS6* with the occurrence of aberrant transcripts at the 3′ region of *SMN1/RPS6*. These mutations suppressed the dwarf, autoimmune phenotypes of the *mekk1* and *mpk4* mutants. We assume that *smn2*-dependent suppression of the autoimmune phenotypes caused by disruption of the MEKK1–MKK1/MKK2–MPK4 pathway was mediated through the loss of function of *SMN1/RPS6*. This suggests that *SMN2/HEN2* plays a novel role in innate immunity by regulating proper *SMN1/RPS6* gene expression.

In conclusion, we showed that the DEAD-box RNA helicase SMN2/HEN2 is involved in the dwarf, autoimmune phenotypes of *mekk1* and *mpk4*. *SMN2/HEN2* is also required for disease resistance mediated by *SMN1/RPS6*. We here revealed novel lines of evidence for the involvement of the nuclear RNA exosome in plant immunity via SMN2/HEN2. A genome-wide approach to isolate RNAs bound to SMN2/HEN2 and to elucidate the dynamics of the SMN2/HEN2-bound RNA population before and after pathogen inoculation would allow us to better understand the function of SMN2/HEN2 in innate immunity. This strategy would also be crucial for unraveling novel aspects of innate immunity from the viewpoint of posttranscriptional gene regulation in plants.

## Materials and Methods

### Plant materials, growth conditions, mutant isolation and MutMap analysis

*Arabidopsis thaliana* plants were grown at 22°C under a 16-h light/8-h dark photoperiod in soil or on solid GM medium supplemented with 1% sucrose unless otherwise stated. We used the Landsberg *erecta* (*Ler*) accession as WT plants. The mutants in the *Ler* background were kindly provided by H. Vaucheret (*hen2-1*), Cold Spring Harbor Laboratory (*mekk1-10*; CSHL DsGT_19053) and H. Hirt (*mpk4-1*; CS5205). To generate the double mutants *mekk1-10smn2-85*, *mekk1-10smn2-90* and *mekk1-10hen2-1*, *mekk1-10* was crossed with *smn2-85*, *smn2-90* or *hen2-1*, respectively. To generate the double mutants *mpk4-1smn2-85* and *mpk4-1hen2-1*, *mpk4-1* was crossed with *smn2-85* or *hen2-1*, respectively. Mutant isolation and MutMap analysis are described in Takagi et al. (2019).

### Construction of transgenic plants carrying the *SMN2/HEN2* promoter::*GUS* construct

A genomic DNA fragment of *SMN2/HEN2* containing 1,634 bp of the 5′ region from the initiation codon was amplified by PCR and cloned into pBI101, which carries the *GUS* coding sequence but no promoter, using the *Hin*dIII and *Xba*I sites with the In-Fusion HD Cloning Kit (Takara Bio, Otsu, Shiga, Japan). The construct was verified by sequencing and used to transform *Ler* by the floral dip method (Clough and Bent 1998). Transformants were selected on GM medium containing 50 μg/ml kanamycin and subjected to histochemical GUS assay.

### Pathogen and plant inoculation

*Pst* strain DC3000 carrying the empty vector pML123 and *Pst* DC3000 (*hopA1*) carrying the plasmid pLN92 expressing *hopA1* from *P. syringae* strain 61 were kindly provided by Gassmann (2005). Plants were grown in soil at 22°C under an 8-h light/16-h dark photoperiod for 6–8 weeks. Rosette leaves were infiltrated with a bacterial suspension of $1 \times 10^5$ colony-forming units (cfu)/ml [*Pst* DC3000 (*hopA1*)] or $5 \times 10^4$ cfu/ml (*Pst* DC3000) in sterilized distilled water (sDW) using a needleless syringe. Leaf disks (φ 4 mm) were excised on days 0 and 3 after inoculation and crushed in sDW. The homogenates were serially diluted with sDW, plated on selective medium and incubated at 28°C for 2 d.

### Staining tissues with X-gluc, trypan blue and DAB

Plants were grown at 22°C for 21 d or 26°C for 14 d on GM medium. Leaves or whole plants were stained with X-gluc for the GUS assay, trypan blue or DAB (all reagents from Sigma-Aldrich, St. Louis, MO, USA) and observed as in Ichimura et al. (2006).

### RT-qPCR analysis

Plants were grown for 14 d on GM medium at 22°C. Total RNA was isolated from whole plants with a Sepazol RNA I Super G reagent (Nacalai Tesque, Kyoto, Japan) according to the manufacturer's instructions. First-strand cDNA was synthesized using ReverTra Ace qPCR RT MasterMix with gDNA Remover (Toyobo, Osaka, Japan). RT-qPCR was performed using a StepOnePlus Real-Time PCR system (Applied Biosystems, Foster City, CA, USA) or a CFX Connect Real-Time System (Bio-Rad Laboratories, Hercules, CA, USA) with primers listed in **Supplementary Table S4**. *Arabidopsis Actin2* was used as an internal control. Relative expression values were calculated using the ddCt method.

### RNA-seq analysis

Two biological replicates of the WT plants and the *smn2-90* mutant were used for cDNA library construction and sequencing. Plants were grown for 14 d on GM medium at 22°C. Total RNA was isolated from whole plants with a NucleoSpin RNA Plant Kit (Takara Bio) according to the manufacturer's instructions. A Dynabeads mRNA Purification Kit was used to purify mRNA, and an Ion Total RNA-Seq Kit v2 was used to construct cDNA libraries (both kits from Thermo Fisher Scientific, Beverly, MA, USA). The quality of total RNA, mRNA and cDNA libraries was analyzed with an Agilent TapeStation (Agilent Technologies, Santa Clara, CA, USA). The cDNA libraries were pooled for emulsion PCR using an Ion PI Hi-Q Chef Kit (Thermo Fisher Scientific). The enriched samples were loaded onto an Ion PI chip v3 with Ion Chef and sequenced with an Ion Proton instrument (Thermo Fisher Scientific). The raw reads from the libraries were filtered to remove adaptor sequences and low-quality bases, and the clean reads from each library were mapped to the reference *Arabidopsis* genome (TAIR 10) using CLC Genomics Workbench (version 9.0; CLC Bio, Aarhus, Denmark). Expression values were measured as RPKM (reads per kilobase of the transcript per million mapped reads). Statistical significance of the differences in gene expression was assessed by comparing the RPKM values using the empirical analysis of digital gene expression in R (edgeR) test (Robinson et al. 2010). The raw sequence reads were deposited in the National Center for Biotechnology Information (**http://www.ncbi.nlm.nih.gov/**) under the accession number GSE143520. GO enrichment analysis was performed by the agriGO (version 2.0) software (**http://systemsbiology.cau.edu.cn/agriGOv2/**) (Tian et al. 2017).

## Supplementary Data

**Supplementary data** are available at PCP online.

## Acknowledgments

We thank Alexander Graf, David Greenshields, Catarina Casais, Kaori Takizawa and Gang-Su Hyon for technical assistance; Dr. Walter Gassmann for providing *Pseudomonas* strains; Dr. Hervé Vaucheret for providing *hen2-1* seeds; Dr. Keiichi Mochida for data analysis; and Drs. Mitsuru Akita and Susumu Mochizuki for discussion. We thank Prof. Nam-Hai Chua of Rockefeller University, New York, for providing the pER8 vector. We also acknowledge the technical expertise of the Gene Research Center facility, Kagawa University.

## Funding

Gatsby Charitable Foundation (to K.S.); UK Biotechnology and Biological Sciences Research Council (to K.S.); Japan Society for the Promotion of Science (JSPS) Postdoctoral Fellowships for Research Abroad (to K.I.); JSPS KAKENHI [19770045, 22780037, 25450060, 19K06054 to K.I.]; JSPS KAKENHI Grant Number 16H06279 (PAGS) (to K.I.); Next Generation Leading Research Fund for 2017 and 2018 of Kagawa University Research Promotion Program (KURPP) (to K.I.); Cooperative Research Grant of the Genome Research for BioResource, NODAI Genome Research Center, Tokyo University of Agriculture (to K.I.); and Sasakawa Scientific Research Grant from The Japan Science Society (to M.T.).

## Disclosures

The authors have no conflicts of interest to declare.

## References

Abe, A., Kosugi, S., Yoshida, K.K., Natsume, S., Takagi, H., Kanzaki, H., et al. (2012) Genome sequencing reveals agronomically important loci in rice using MutMap. *Nat. Biotechnol.* 30: 174–178.

Asai, S. and Shirasu, K. (2015) Plant cells under siege: plant immune system versus pathogen effectors. *Curr. Opin. Plant Biol.* 28: 1–8.

Asai, T., Tena, G., Plotnikova, J., Willmann, M.R., Chiu, W., Gomez-Gomez, L., et al. (2002) MAP kinase signalling cascade in Arabidopsis innate immunity. *Nature* 415: 977–983.

Aubourg, S., Kreis, M., Lecharny, A., Biotechnologie, I.D. and Biologie, L.D. (1999) The DEAD box RNA helicase family in *Arabidopsis thaliana*. *Nucleic Acids Res.* 27: 628–636.

Cheng, Y., Kato, N., Wang, W., Li, J. and Chen, X. (2003) Two RNA binding proteins, HEN4 and HUA1, act in the processing of *AGAMOUS* pre-mRNA in *Arabidopsis thaliana*. *Dev. Cell* 4: 53–66.

Chiba, Y. and Green, P.J. (2009) mRNA degradation machinery in plants. *J. Plant Biol.* 52: 114–124.

Clough, S.J. and Bent, A.F. (1998) Floral dip: a simplified method for *Agrobacterium*-mediated transformation of *Arabidopsis thaliana*. *Plant J.* 16: 735–743.

Cui, H., Tsuda, K. and Parker, J.E. (2015) Effector-triggered immunity: from pathogen perception to robust defense. *Annu. Rev. Plant Biol.* 66: 487–511.

del Pozo, O., Pedley, K.F. and Martin, G.B. (2004) MAPKKK$\alpha$ is a positive regulator of cell death associated with both plant immunity and disease. *EMBO J.* 23: 3072–3082.

Dodds, P.N. and Rathjen, J.P. (2010) Plant immunity: towards an integrated view of plant–pathogen interactions. *Nat. Rev. Genet.* 11: 539–548.

Gassmann, W. (2005) Natural variation in the Arabidopsis response to the avirulence gene *hopPsyA* uncouples the hypersensitive response from disease resistance. *Mol. Plant Microbe Interact.* 18: 1054–1060.

Gloggnitzer, J., Akimcheva, S., Srinivasan, A., Kusenda, B., Riehs, N., Stampfl, H., et al. (2014) Nonsense-mediated mRNA decay modulates immune receptor levels to regulate plant antibacterial defense. *Cell Host Microbe* 16: 376–390.

Hématy, K., Bellec, Y., Podicheti, R., Bouteiller, N., Anne, P., Morineau, C., et al. (2016) The zinc-finger protein SOP1 is required for a subset of the nuclear exosome functions in Arabidopsis. *PLoS Genet.* 12: e1005817.

Hong, K.Y., Lee, S.H., Gu, S., Kim, E., An, S., Kwon, J., et al. (2017) The bent conformation of poly(A)-binding protein induced by RNA-binding is required for its translational activation function. *RNA Biol.* 14: 370–377.

Ichimura, K., Casais, C., Peck, S.C., Shinozaki, K. and Shirasu, K. (2006) MEKK1 is required for MPK4 activation and regulates tissue-specific and temperature-dependent cell death in *Arabidopsis*. *J. Biol. Chem.* 281: 36969–36976.

Ichimura, K., Mizoguchi, T., Irie, K., Morris, P., Giraudat, J., Matsumoto, K., et al. (1998) Isolation of ATMEKK1 (a MAP kinase kinase kinase)—interacting proteins and analysis of a MAP kinase cascade in *Arabidopsis*. *Biochem. Biophys. Res. Commun.* 253: 532–543.

Jensen, T.H. (2010) *RNA Exosome, Advances in Experimental Medicine and Biology*. Springer-Verlag, New York, NY.

Kim, S.H., Kwon, S.I., Saha, D., Anyanwu, N.C. and Gassmann, W. (2009) Resistance to the *Pseudomonas syringae* effector HopA1 is governed by the TIR-NBS-LRR protein RPS6 and is enhanced by mutations in *SRFR1*. *Plant Physiol.* 150: 1723–1732.

Kong, Q., Qu, N., Gao, M., Zhang, Z., Ding, X., Yang, F., et al. (2012) The MEKK1-MKK1/MKK2-MPK4 kinase cascade negatively regulates immunity mediated by a mitogen-activated protein kinase kinase kinase in *Arabidopsis*. *Plant Cell* 24: 2225–2236.

Kovtun, Y., Chiu, W., Tena, G. and Sheen, J. (2000) Functional analysis of oxidative stress-activated mitogen-activated protein kinase cascade in plants. *Proc. Natl. Acad. Sci. USA* 97: 2940–2945.

Lange, H., Sement, F.M. and Gagliardi, D. (2011) MTR4, a putative RNA helicase and exosome co-factor, is required for proper rRNA biogenesis and development in *Arabidopsis thaliana*. *Plant J.* 68: 51–63.

Lange, H., Zuber, H., Sement, F.M., Chicher, J., Kuhn, L., Hammann, P., et al. (2014) The RNA helicases AtMTR4 and HEN2 target specific subsets of nuclear transcripts for degradation by the nuclear exosome in *Arabidopsis thaliana*. *PLoS Genet.* 10: e1004564.

Lian, K., Gao, F., Sun, T., van Wersch, R., Ao, K., Kong, Q., et al. (2018) MKK6 functions in two parallel MAP kinase cascades in immune signaling. *Plant Physiol.* 178: 1284–1295.

Lyons, R., Iwase, A., Gänsewig, T., Sherstnev, A., Duc, C., Barton, G.J., et al. (2013) The RNA-binding protein FPA regulates flg22-triggered defense responses and transcription factor activity by alternative polyadenylation. *Sci. Rep.* 3: 2866.

Pause, A., Méthot, N. and Sonenberg, N. (1993) The HRIGRXXR region of the DEAD box RNA helicase eukaryotic translation initiation factor 4A is required for RNA binding and ATP hydrolysis. *Mol. Cell. Biol.* 13: 6789–6798.

Qiu, J., Zhou, L., Yun, B., Nielsen, H.B., Fiil, B.K., Petersen, K., et al. (2008) Arabidopsis mitogen-activated protein kinase kinases MKK1 and MKK2 have overlapping functions in defense signaling mediated by MEKK1, MPK4, and MKS1. *Plant Physiol.* 148: 212–222.

Ranf, S. (2017) Sensing of molecular patterns through cell surface immune receptors. *Curr. Opin. Plant Biol.* 38: 68–77.

Robinson, M.D., McCarthy, D.J. and Smyth, G.K. (2010) edgeR: A bioconductor package for differential expression analysis of digital gene expression data. *Bioinformatics* 26: 139–140.

Roux, M.E., Rasmussen, M.W., Palma, K., Lolle, S., Mateu, À., Bethke, G., et al. (2015) The mRNA decay factor PAT1 functions in a pathway including MAP kinase 4 and immune receptor SUMM2. *EMBO J.* 34: 593–608.

Sikorska, N., Zuber, H., Gobert, A., Lange, H. and Gagliardi, D. (2017) RNA degradation by the plant RNA exosome involves both phosphorolytic and hydrolytic activities. *Nat. Commun.* 8: 2162.

Suarez-Rodriguez, M.C., Petersen, M. and Mundy, J. (2010) Mitogen-Activated Protein Kinase Signaling in Plants. *Annu. Rev. Plant Biol.* 61: 621–649.

Sun, H.-X., Li, Y., Niu, Q.-W. and Chua, N.-H. (2017) Dehydration stress extends mRNA 3′ untranslated regions with noncoding RNA functions in *Arabidopsis*. *Genome Res.* 27: 1427–1436.

Takagi, M., Hamano, K., Takagi, H., Morimoto, T., Akimitsu, K., Terauchi, R., et al. (2019) Disruption of the MAMP-induced MEKK1-MKK1/MKK2- MPK4 pathway activates the TNL immune receptor SMN1/RPS6. *Plant Cell Physiol.* 60: 778–787.

Tarun, S.Z. and Sachs, A.B. (1996) Association of the yeast poly(A) tail binding protein with translation initiation factor eIF-4G. *EMBO J.* 15: 7168–7177.

Tian, T., Liu, Y., Yan, H., You, Q., Yi, X., Du, Z., et al. (2017) AgriGO v2.0: a GO analysis toolkit for the agricultural community, 2017 update. *Nucleic Acids Res.* 45: W122–W129.

Tsuda, K. and Katagiri, F. (2010) Comparing signaling mechanisms engaged in pattern-triggered and effector-triggered immunity. *Curr. Opin. Plant Biol.* 13: 459–465.

Western, T.L., Cheng, Y., Liu, J. and Chen, X. (2002) HUA ENHANCER2, a putative DExH-box RNA helicase, maintains homeotic B and C gene expression in Arabidopsis. *Development* 129: 1569–1581.

Xi, L., Moscou, M.J., Meng, Y., Xu, W., Caldo, R.A., Shaver, M., et al. (2009) Transcript-based cloning of RRP46, a regulator of rRNA processing and *R* gene-independent cell death in barley-powdery mildew interactions. *Plant Cell* 21: 3280–3295.

Zhang, X. and Guo, H. (2017) mRNA decay in plants: both quantity and quality matter. *Curr. Opin. Plant Biol.* 35: 138–144.

Zhang, Z., Liu, Y., Huang, H., Gao, M., Wu, D., Kong, Q., et al. (2017) The NLR protein SUMM2 senses the disruption of an immune signaling MAP kinase cascade via CRCK3. *EMBO Rep.* 18: 292–302.

Zhang, Z., Wu, Y., Gao, M., Zhang, J., Kong, Q., Liu, Y., et al. (2012) Disruption of PAMP-induced MAP kinase cascade by a *Pseudomonas syringae* effector activates plant immunity mediated by the NB-LRR protein SUMM2. *Cell Host Microbe* 11: 253–263.